Dry Redox Reforming Hybrid Power Cycle: Performance Analysis and Comparison to Steam Redox Reforming

Elysia J. Sheu[a], Esmail M. A. Mokheimer[b], Ahmed F. Ghoniem[a,*]

[a] *Department of Mechanical Engineering, Massachusetts Institute of Technology, 77 Massachusetts Avenue, Cambridge, MA, USA*
[b] *Department of Mechanical Engineering, King Fahd University of Petroleum and Minerals, Dhahran 31261, Saudi Arabia*

Abstract

There has been much interest in the use of renewable resources for power generation as the world's energy demand and the concern over the rise in emissions increases. In the near term, however, renewable sources such as solar energy are expected to provide a small fraction of the world's energy demand due to intermittancy and storage problems. A potential solution is the use of hybrid solar-fossil fuel power generation. Previous work has shown the potential of steam redox reforming for hybridization. However, this type of reforming requires some water consumption (which may be infeasible in certain locations) as not all the water can be recovered through recycling. An alternative is to utilize dry (or CO_2) redox reforming. In this paper, a system analysis for a CO_2 redox reforming hybrid cycle and comparison of cycle and reformer performance between a CO_2 redox reformer and steam redox reformer hybrid cycle are presented. The effect of important operating parameters such as pressure, amount of reforming CO_2, and the oxidation temperature on the reformer and cycle performance are discussed. Simulation results show that increasing the oxidation temperature or the amount of reforming CO_2 leads to higher reformer and

*Corresponding Author: ghoniem@mit.edu, Tel: +1 6172532295, Fax: +1 6172535981

cycle efficiencies. In addition, the comparison between the CO_2 and steam redox reformer hybrid cycles shows that the CO_2 cycle has the potential to have better overall performance.

Keywords: Hybrid Solar-Fossil Fuel, System Analysis, Solar Reforming, Thermodynamic Analysis, Chemical Looping, Dry Redox

---

Nomenclature

Latin Letters

HRSG	Heat Recovery Steam Generator	
ΔH^o	Standard Enthalpy of Reaction	kJ/mol
$X_{input,solar}$	Input Solar Share	
Q	Heat Input	W
I	Solar Irradiance	W/m^2
A	Solar Collector Area	m^2
T	Temperature	K
$\tilde{C}$	Mean Flux Concentration Ratio	suns
$\dot{n}$	Molar Flow Rate	mol/s

Greek Letters

σ	Stefan-Boltzmann Constant	$W/m^2/K^4$
η	Efficiency	

Subscripts

red	Reduction
oxd	Oxidation
$solar$	Solar Field Input
$fuel$	Fuel Input
ref	Reformer
rec	Solar Receiver
$chem$	Chemical

1. Introduction

With concern regarding emissions due to fossil fuel power production growing, there is an increased interest in using renewable resources such as solar for power production. However in the near term, due to intermittency and storage issues, renewable resources like solar are expected to provide minimal contribution to the world's energy demand [1]. One potential solution for these problems is hybrid solar-fossil fuel power generation. With the hybrid operation, intermittency concerns are eliminated as fuel can be used when solar is not available, and in particular, when solar reforming is used as the hybridization method, a viable storage option is obtained through the use of solar fuels [2]. Moreover, analysis of solar reforming hybrid cycles has shown that the hybridization can improve the solar energy system performance [3].

When solar reforming is used as the hybridization technique, fuel (natural gas) is reformed into syngas (which has a higher heating value) using the solar energy. The

produced syngas is then used as the fuel for a gas turbine system. Many different reforming processes can be used to convert the natural gas into syngas. These processes include steam reforming, CO_2 (dry) reforming, and to a lesser extent, metal redox reforming.

There has been much previous work on solar steam and dry reformers [4, 5, 6, 7, 8, 9, 10, 11] as well as redox reformers [12, 13, 14, 15, 16, 17]. System level studies have also been performed for steam and redox reformer hybrid cycles [2, 3, 18]. Specifically for the redox reformer hybrid cycle, the previous analysis done was for a reformer utilizing steam in the oxidation step [18]. The system analysis of the steam redox reformer cycle identified important parameters, such as amount of reforming water and oxidation temperature, and their effect on both reformer and cycle performance.

A hybrid cycle that utilizes this steam redox reforming requires consumption of steam since not enough water can be obtained through just recycling. Another option is to use CO_2 instead of steam within the redox reformer. If CO_2 is used as the oxidizing agent, the main reactions for the reformer are

$$MO + CH_4 \rightarrow M + CO + 2H_2 \text{ (Endothermic)}$$

$$M + CO_2 \rightarrow MO + CO \text{ (Exothermic or Endothermic)}$$

where M/MO represents the metal/metal oxide pair chosen for the redox reactions.

Geographic locations that have large solar energy resources usually also have water scarcity and may not have the water needed to operate a steam redox reforming hybrid cycle that requires some water consumption. Therefore, it would be useful to determine what conditions would be needed for a redox reformer hybrid cycle that utilizes CO_2 and how its performance compares to that of the steam redox

reformer hybrid cycle. In this paper, a system level analysis of a CO_2 based redox reformer hybrid power cycle is presented. The effect of pressure, amount of reforming CO_2 used, reformer temperature, and solar energy fraction on the redox reformer and hybrid cycle performance is discussed. In addition, the performance of this type of hybrid cycle is compared to that of the redox reformer hybrid cycle that utilizes steam. The performance is compared on the basis of both reformer and cycle performance. Moreover, the operating conditions for the metal redox reforming processes (using either steam or CO_2 for oxidation) are discussed.

2. Metal Redox Reforming Conditions

Before going into the detail regarding the system analysis, the operating conditions for the redox reforming process will be presented. As shown previously, metal redox reforming involves a two step process. First, a fuel (methane) is used to reduce a metal oxide, forming metal (or a reduced state of a metal oxide) and syngas. Next, the reduced metal is oxidized using an oxidizing agent (air, steam, or CO_2). Basically, a chemical looping process is created. From previous system analysis of a redox reforming hybrid cycle, iron/magnetite was shown to be a promising metal/metal oxide pair for solar redox reforming due to its required temperatures for the reactions, oxygen carrying capacity, and material costs [18]. The iron/magnetite pair will be used for the redox reformer cycle analysis done herein. The reduction and oxidation reactions for the iron/magnetite are

$$\frac{1}{4}\mathrm{Fe_3O_4} + \mathrm{CH_4} \rightarrow \frac{3}{4}\mathrm{Fe} + \mathrm{CO} + 2\mathrm{H_2} \quad \Delta H^o = 243.93\mathrm{kJ/mol}$$

$$\frac{3}{4}\mathrm{Fe} + \mathrm{CO_2} \rightarrow \frac{1}{4}\mathrm{Fe_3O_4} + \mathrm{CO} \quad \Delta H^o = 3.23\mathrm{kJ/mol}$$

Note that the oxidation reaction with CO_2 is slightly endothermic which is different from oxidation with steam which is exothermic [18].

The methane conversion as a function of temperature for the reduction reaction is shown in Figure 1.

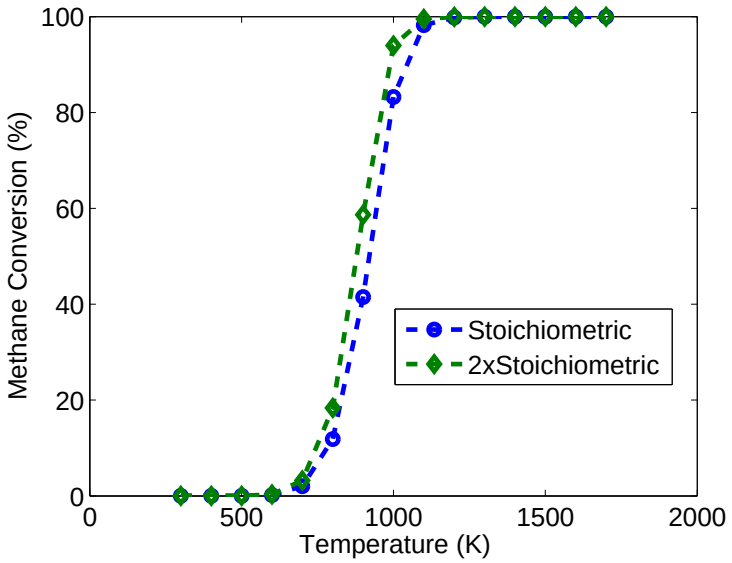

Figure 1: Equilbrium Methane Conversion for Fe_3O_4 Reduction at Different Temperatures (Stoichiometric and 2 x Stoichiometric Metal Oxide to Fuel Ratio)

The methane conversion at equilibrium is determined using the equilibrium constants (Table 1) calculated using Gibbs free energy of formation values found in [19].

From Figure 1, it can be seen that higher temperatures are preferred in terms of methane conversion ($>$ 1050K for complete conversion). Moreover, increasing the metal oxide to fuel ratio decreases the temperature required for complete conversion. Increasing this ratio increases material costs; however, it helps decrease the solar collector cost as it lowers the required temperatures.

The pressure dependence of methane conversion for the reduction reaction is shown in Figure 2. Lower pressures are preferred for methane conversion because volume expansion occurs during the reduction step.

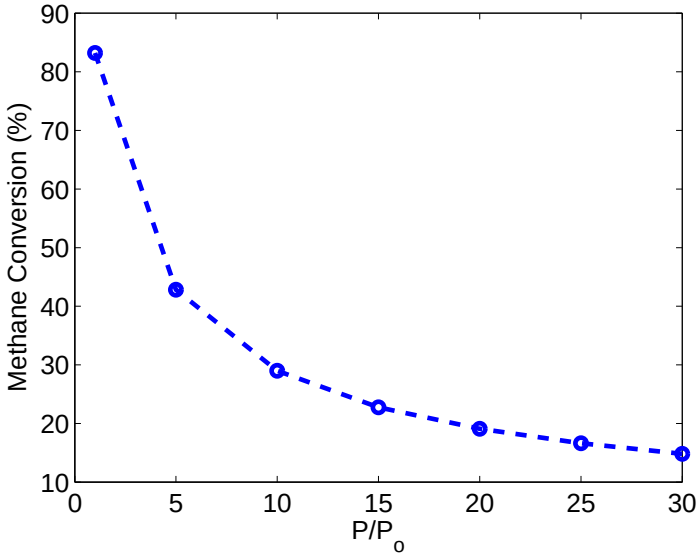

Figure 2: Equilibrium Methane Conversion for Fe_3O_4 reduction at Different Pressures (Stoichiometric metal oxide to fuel ratio)

In the oxidation reaction, the main goal is to convert all the metal to metal oxide (and producing CO). Iron oxidation results are shown in Figure 3, determined using the equilibrium constants (Table 1) calculated from the Gibbs free energy of reaction found in [19]. For comparison, the iron oxidation results are plotted with the steam oxidation results obtained from [18].

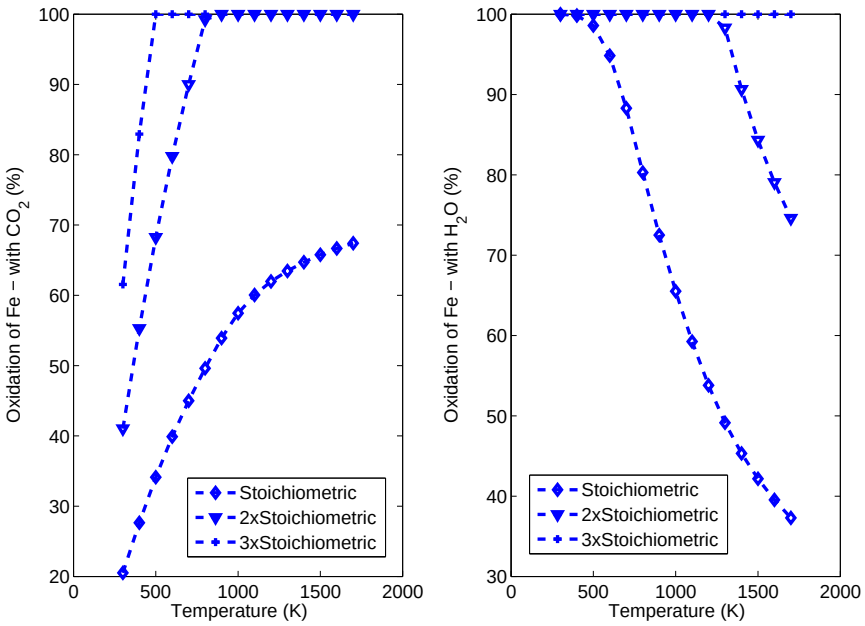

Figure 3: Equilibrium Iron Oxidation Using CO_2 (Left) and Steam (Right) for different steam/CO_2 to iron ratios

Figure 3 shows that the oxidation of Fe with CO_2 favors higher temperature given that the reaction is endothermic ($>$ 800K for complete conversion when 2 x stoichiometric amount is used). Moreover, higher than stoichiometric amounts of CO_2 are required in order to ensure that all metal is oxidized at reasonable temperatures. Figure 3 also shows that the oxidation with steam favors lower temperatures because the oxidation reaction with steam is exothermic. In addition, super-stoichiometric amounts of water allow for complete conversion of Fe over a wider range of temperatures, which is important as the operating temperatures are likely to be higher in order for the reactions to proceed at a reasonable rate [18].

Because in the oxidation reaction (with either steam or CO_2) there is no change in the number of moles of gas from the reactants to the products, there is no pressure

Temperature (K)	K_p-Reduction	K_p-Oxidation
300	8.66e-30	0.26
400	4.13e-19	0.38
500	1.22e-12	0.52
600	2.69e-8	0.66
700	3.49e-5	0.82
800	7.56e-3	0.98
900	0.49	1.17
1000	13.74	1.35
1100	212.96	1.50
1200	2.10e3	1.63
1300	1.46e4	1.74
1400	7.67e4	1.83
1500	3.21e5	1.92
1600	1.12e6	2.00
1700	3.36e6	2.07

Table 1: Equilibrium Constants at Different Temperatures for Fe_3O_4 Reduction Reaction with Methane and Fe Oxidation Reaction with CO_2

dependence for the iron metal conversion at equilibrium.

Overall, for the reduction of magnetite, higher temperatures and lower pressures are preferred. For the oxidation of iron with CO_2, higher temperatures are preferred (with higher than stoichiometric amounts of CO_2 required for complete conversion at reasonable temperatures) while for oxidation with steam, lower temperatures are preferred (at least in terms of equilibrium).

Now that the reforming conditions have been discussed, the hybrid power cycle model will be described next.

3. Hybrid Power Cycle Model

A schematic of the hybrid cycle analyzed herein is shown in Figure 4. The hybrid power cycle used in this analysis is similar to the one used in [18] and consists of

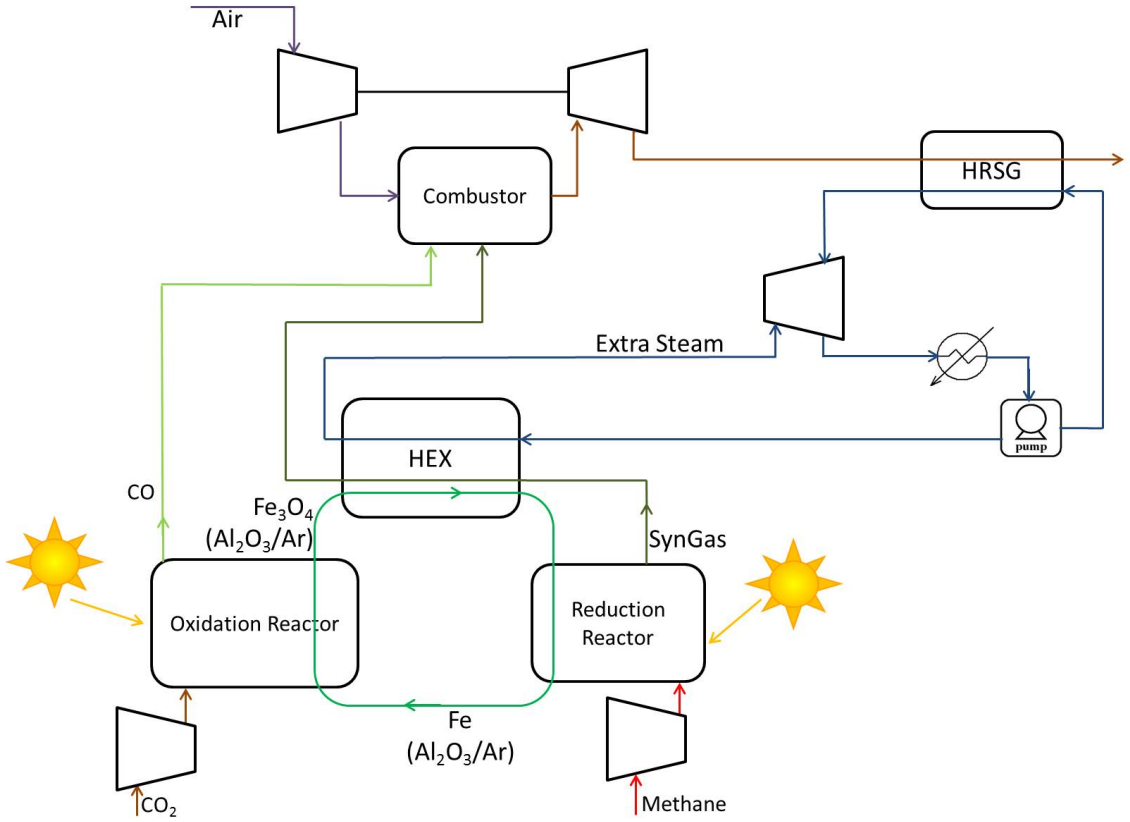

Figure 4: Schematic CO_2 Redox Reforming Cycle

the reformer system and a combined cycle with a triple pressure heat recovery steam generator (HRSG). For the redox reformer, Alumina is chosen as the support material of the oxygen carrier and Argon is chosen as the carrier gas of the circulating oxygen carrier. The Alumina support flow rate is chosen such that the metal is 60% of the total metal/support mass. The redox reformer system is modeled as two separate reactors with the iron/magnetite/Alumina/Ar circulating between the two reactors. The CO_2 for reforming is assumed to be readily available. The implementation of the solar collector system with the two reactors is similar to the one presented in

[18] in that the solar application is modeled as a heat source. Since, as discussed previously, the oxidation of Fe with CO_2 is endothermic, both the oxidation and reduction reactor utilizes the solar energy. For all simulations, unless otherwise noted, 25% of the solar energy input is used in the oxidation reactor and the rest is used in the reduction reactor. This percentage was chosen so that the range of oxidation temperatures achieved were suitable for complete conversion of the iron. Both reduction and oxidation reactors are modeled as equilibrium reactors.

Parameter	**Value(s)**
Methane Input	0.125 kmol/s
Gas Turbine Inlet Temperature	1600 K
HRSG High Pressure	85 bar
High Pressure Steam Temperature	700 K
HRSG Intermediate Pressure	25 bar
Intermediate Pressure Steam Temperature	600 K
HRSG Low Pressure	5 bar
Low Pressure Steam Temperature	500 K
Isentropic Efficiency - Turbine	95%
Isentropic Efficiency - Compressor	90%
Metal Oxide Flow Rate	0.032 kmol/s
Alumina Support Flow Rate	0.0484 kmol/s
Carrier Gas Flow Rate (Ar)	0.281 kmol/s
Steam Cycle Flow Rate	0.8 - 1.35 kmol/s
Air Flow Rate	2.5 - 3.5 kmol/s
Reforming CO_2	0.25 or 0.375 kmol/s
Combustor/Reformer Pressure	10, 20, or 30 bar
Oxidation Reactor Temperature	650 - 960 K
Reduction Reactor Temperature	800 - 1020 K

Table 2: Operating Conditions for Hybrid Cycle

Table 2 shows the operating parameters of the hybrid cycle. The reduction reactor outlet (including the syngas product as well as the iron/magnetite/Alumina/Ar mixture) is cooled create additional steam for the steam cycle. After cooling, the

syngas is sent to the combustor and the solid/carrier gas mixture is sent to the oxidation reactor. For the oxidation reactor, the generated CO is sent to the combustor similar to the syngas created from the reduction reactor. The methane input is kept the same for all simulations.

The metal oxide flow rate is chosen to be slightly higher than the stoichiometric amount because in practical operation not all metal oxide is available for the reforming process. The nominal stoichiometric amount of metal oxide (0.032 kmol/s) is chosen for the analysis herein based on the results presented in [18].

The modeling of the power cycle including the combustor, HRSG, etc. is the same as the one presented in [18]. The hybrid cycle is modeled in Aspen Plus. How the cycle model is analyzed and the comparison of cycle and reformer performance to that of the cycle presented in [18] will be presented next.

4. System Analysis Results

The hybrid cycle is simulated for a large range of input solar shares. The "input solar share" is defined as

$$X_{input,solar} = \frac{\dot{Q}_{solar}}{\dot{Q}_{solar} + \dot{Q}_{fuel}}$$

where $\dot{Q}_{fuel}$ is the fuel input and $\dot{Q}_{solar}$ is the solar energy input. $\dot{Q}_{solar}$ is the total amount of solar energy available (before taking into account any receiver or reforming losses) and is defined as

$$\dot{Q}_{solar} = IA$$

where I is the solar irradiance (in W/m^2) and A is the solar collector area.

The hybrid cycle performance is evaluated based on reformer and cycle efficiency.

The reformer efficiency is defined as

$$\eta_{ref} = \eta_{rec}\eta_{chem}$$

where η_{ref} is the overall reformer system efficiency, η_{rec} is the receiver efficiency defined as

$$\eta_{rec} = 1 - \left(\frac{\sigma T^4}{I\tilde{C}}\right)$$

and η_{chem} is the "chemical" efficiency and is defined as

$$\eta_{chem} = \frac{-\dot{n}_p \Delta H_p|_{T_p}}{-\dot{n}_r \Delta H_r|_{T_r} + \dot{Q}_{rec}}$$

For the receiver efficiency, σ is the Stefan-Boltzmann constant, T is the receiver temperature (reformer temperature), and $\tilde{C}$ is the mean flux concentration ratio. This receiver efficiency is based on assuming that the receiver reformer is a black body and that heat losses are mainly due to radiation [20]. For the analysis herein, a value of 2500 suns is used for $\tilde{C}$ and I is fixed at 600 W/m^2.

For the chemical efficiency, $\Delta H_p|_{T_p}$ and $\Delta H_r|_{T_r}$ is the enthalpy of the reformer products and reactants at product temperature T_p and reactant temperature T_r, respectively and $\dot{Q}_{rec}$ is defined as

$$\dot{Q}_{rec} = \eta_{rec}\dot{Q}_{solar}$$

Note that for the chemical efficiency, the temperatures and flow rates for the reactants and products and the $\dot{Q}_{rec}$ include those for both the reduction and oxidation reactor.

The hybrid cycle efficiency is based on the first law cycle efficiency and defined

as

$$\eta_{cycle} = \frac{\dot{W}_{hybrid}}{\dot{Q}_{fuel} + \dot{Q}_{solar}}$$

where $\dot{W}_{hybrid}$ is the work output from the hybrid cycle.

The system analysis results will now be presented.

4.1. Effect of Pressure

To study the effect of pressure on the cycle and reformer efficiency, the hybrid cycle is simulated for three different combustor/reformer operating pressures (10, 20, and 30 bar). 2 times stoichiometric amount of reforming CO_2 is used.

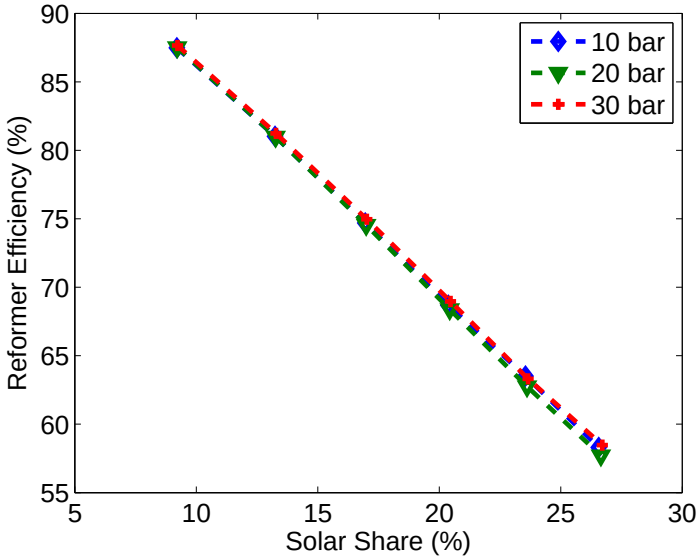

Figure 5: Reformer efficiency at Different Operating Pressures (T_{oxd} = 670 - 850 K)

Figure 5 shows that the operating pressure does not have much effect on the reformer efficiency. As discussed previously, the reduction reaction favors lower pressures for methane conversion, and thus it would be expected that the reformer with

the lower operating pressure would have higher conversion and thus higher reformer efficiency. While the 10 bar reformer does indeed have higher methane conversion (Figure 6), the difference in the level of conversion is not significant enough to lead to a significant difference in reformer efficiency.

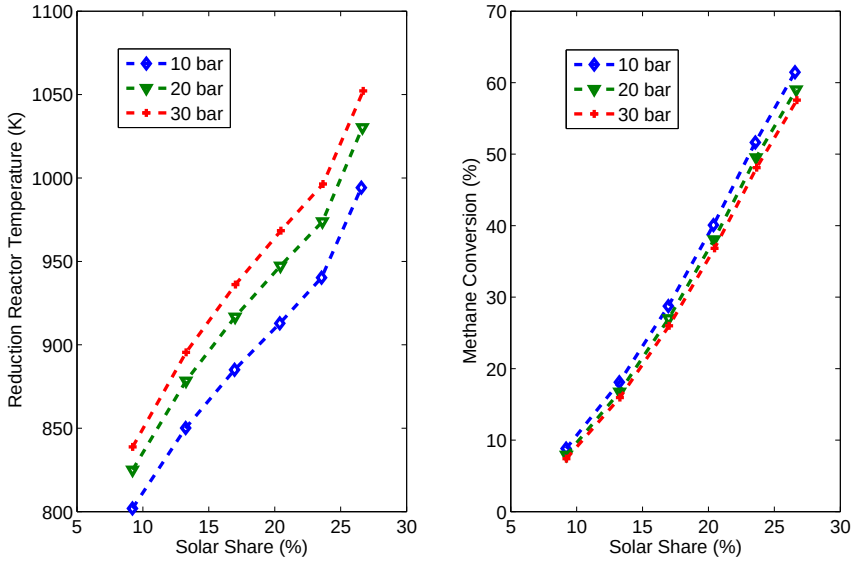

Figure 6: Reduction Reactor Temperature and Methane Conversion for Different Operating Pressures (T_{oxd} = 670 - 850 K)

The reason for this relatively small difference in methane conversion is that the higher operating pressure reformer has the higher operating temperature (Figure 6) which is also favored by the reduction reaction. Thus, despite the differing operating pressure, methane conversion is not that different among the three reformers, which leads to nearly the same reformer efficiencies.

Figure 5 also shows that as solar share increases, the reformer efficiency decreases. The reformer efficiency decreases due to the decreasing receiver and chemical efficiency with the increasing solar share. The drop in receiver efficiency is due to the

higher reforming temperature at higher solar share. The chemical efficiency drops because the rate of increase in reforming gains is not the same as the rate of increase in the solar energy added with increasing solar share. In other words at larger solar share, the higher reforming temperature is not enough to raise the reforming gain.

While the operating pressure did not have much effect on reformer efficiency, it does have a significant effect on the cycle efficiency (Figure 7). Figure 7 shows that increasing the reformer pressure leads to a higher cycle efficiency. This efficiency increase is due to the increase in gas turbine work resulting from the higher operating pressure. Moreover, the increase in cycle efficiency is not as large when going from the 20 to 30 bar case as compared to increasing the operating pressure from 10 to 20 bar. Again, the cycle efficiency decreases with increasing solar share due to the decreasing reformer efficiency.

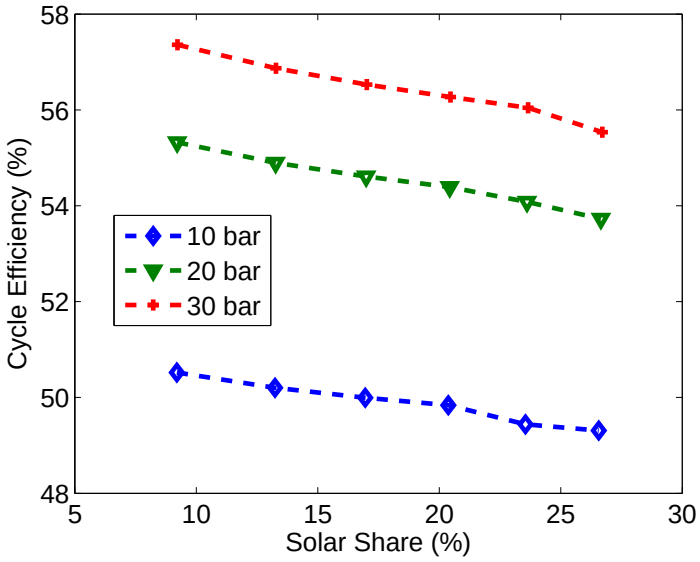

Figure 7: Cycle Efficiency at Different Operating Pressures (T_{oxd} = 670 - 850 K)

In summary increasing the reformer pressure does not have much effect on the

reformer efficiency; however, increasing the reformer pressure does lead to an increase in cycle efficiency. The effect of pressure on reformer performance is similar for the CO_2 redox reformer cycle analyzed here and the steam redox reformer cycle analyzed in [18] in that the reformer pressure does not significantly affect the reformer efficiency and increasing the reformer pressure leads to higher cycle efficiency. Now that the effect of reformer pressure has been investigated, the effect of amount of reforming CO_2 on reformer and cycle performance will be discussed next.

4.2. Effect of Amount of Reforming CO_2 Used

For determining the effect of the amount of reforming CO_2 on both reformer and cycle performance, the hybrid cycle performance is compared for cases when 0.25 kmol/s and 0.375 kmol/s of reforming CO_2 is used (nominally 2 times stoichiometric and 3 times stoichiometric). Note that the stoichiometric amount of CO_2 is not used because as discussed previously, higher than stoichiometric amounts of CO_2 is needed in order to achieve full metal conversion at reasonable temperatures. Also note that since the solar energy utilized in the oxidation reactor (25% of the total solar energy input) is kept the same for both cases, the oxidation temperature range will differ for the two cases due to the differing amounts of reforming CO_2. The combustor/reformer operating pressure is set to 20 bar.

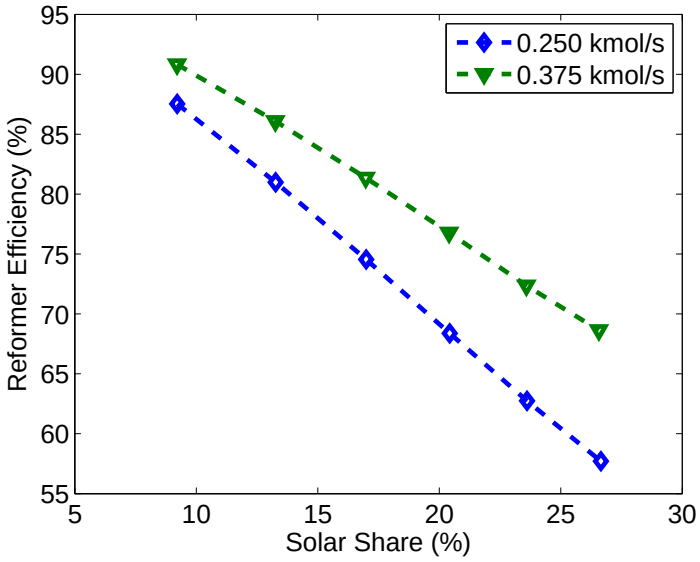

Figure 8: Reformer Efficiency at Different Amounts of Reforming CO_2 (T_{oxd} = 670 - 850 K for 0.250 kmol/s case, T_{oxd} = 650-800 K for 0.375 kmol/s case)

From Figure 8 it can be seen that increasing the amount of reforming CO_2 increases the reformer efficiency. A higher amount of reforming CO_2 leads to lower oxidation temperatures and therefore lower reduction reactor temperatures and methane conversion (Figure 9). However when CO_2 amount is raised, the degree of reforming in the oxidation reactor increases (at equal temperatures - see Figure 3). Therefore the additional reforming gains in the oxidation reactor (from the endothermic reaction of Fe conversion) for the 0.375 kmol/s case are able to counteract the slightly lower reforming gains in the reduction reactor (as compared to the 0.250 kmol/s case - Figure 9), which leads to the higher reformer efficiency for the 0.375 kmol/s case.

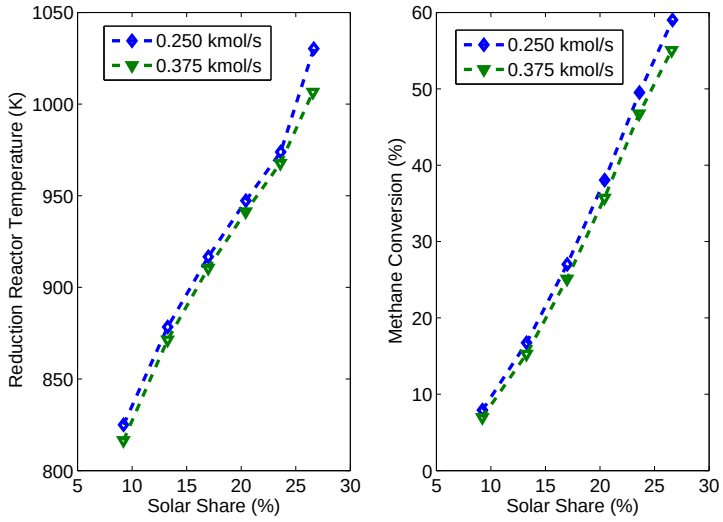

Figure 9: Reduction Reactor Temperature and Methane Conversion for Different Amounts of Reforming CO_2 (T_{oxd} = 670 - 850 K for 0.250 kmol/s case, T_{oxd} = 650-800 K for 0.375 kmol/s case)

The cycle efficiency for the two cases is shown in Figure 10. Because the 0.375 kmol/s case has the higher reformer efficiency the cycle efficiency for the 0.375 kmol/s case is also higher.

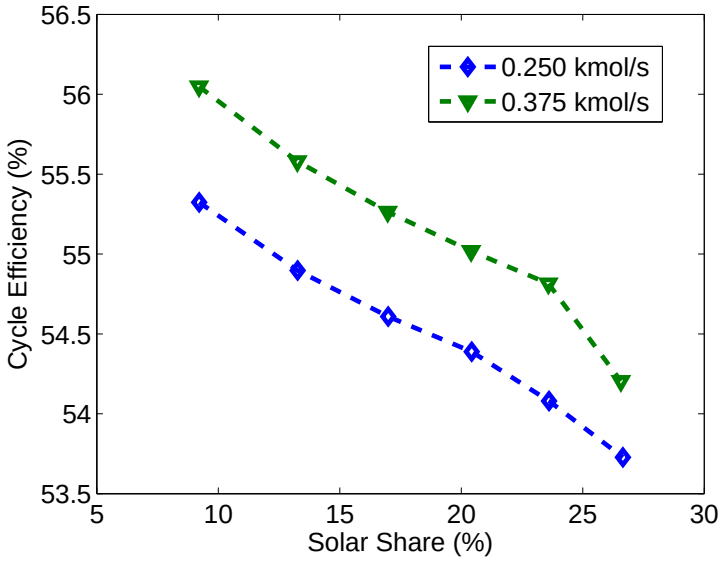

Figure 10: Cycle Efficiency for Different Amounts of Reforming CO_2 (T_{oxd} = 670 - 850 K for 0.250 kmol/s case, T_{oxd} = 650-800 K for 0.375 kmol/s case)

Both the reformer and cycle efficiency decrease with increasing solar share due to the reason discussed previously.

Overall, increasing the reforming CO_2 used leads to better reformer and cycle performance. When compared to the case of steam redox reforming, the effect is the same in that increasing the reforming steam or CO_2 used increases the reformer efficiency. However, while increasing the amount of reforming steam does not significantly affect the steam redox reformer cycle efficiency [18], increasing the amount of reforming CO_2 used raises the cycle efficiency.

However, as mentioned previously, increasing the amount of reforming CO_2 does change the oxidation temperature. The effect of the oxidation temperature on CO_2 redox reformer and cycle performance will be presented next.

4.3. Effect of Oxidation Temperature

To determine the effect of the oxidation temperature on the reformer and cycle performance, the hybrid cycle was simulated using two different temperature ranges for the oxidation temperature. For the higher oxidation temperature case, 35% of the solar energy is used for the oxidation reactor as opposed to the 25% that has been used for all previous simulations. Thus, the two temperature ranges for the oxidation reactor are 670 - 850 K and 710 - 955 K. The reformer operating pressure is set to 20 bar and 2 times stoichiometric amount of CO_2 is used.

First, the comparison between the reformer efficiency for these two temperature cases is shown in Figure 11. The comparison shows that increasing the oxidation

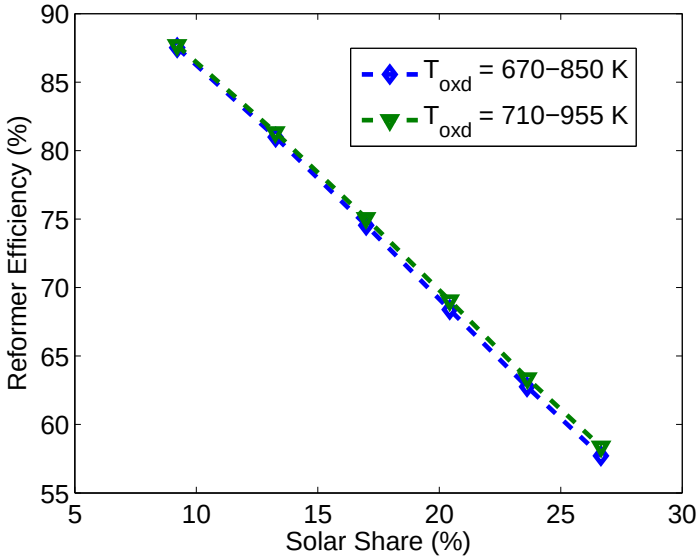

Figure 11: Reformer Efficiency at Different Oxidation Temperatures

temperature leads to a slightly higher reformer efficiency. The higher oxidation temperature leads to a higher reduction reactor inlet temperature; however, from

Figure 12 it can be seen that the higher oxidation temperature case actually has a lower reduction reactor temperature and therefore lower methane conversion.

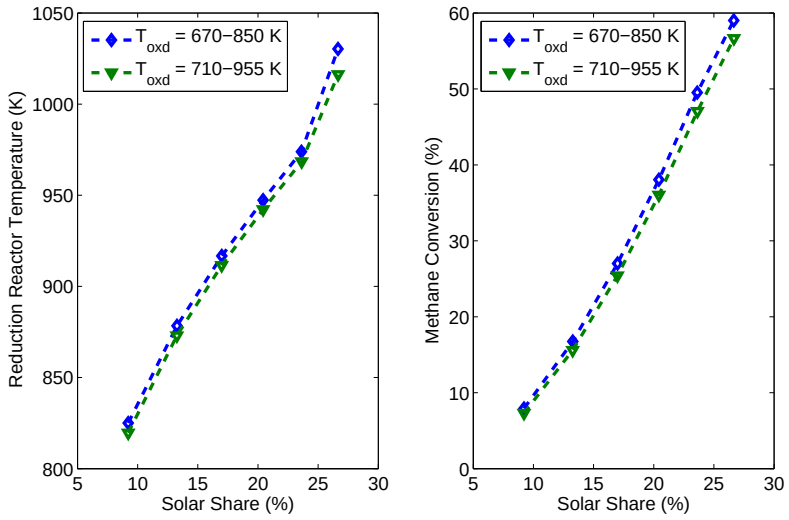

Figure 12: Reduction Reactor Temperature and Methane Conversion for Different Oxidation Temperatures

Even though the inlet temperature is higher for the higher oxidation temperature case, the amount of solar energy available for the reduction reactor is lower which leads to the lower reduction reactor temperature and lower methane conversion. However this slightly lower methane conversion is counteracted by the higher gains in reforming within the oxidation reactor (which is an endothermic reaction) which leads to the slightly higher reformer efficiency for the higher oxidation temperature case.

The corresponding cycle efficiency comparison is shown in Figure 13. Since the higher oxidation temperature case has a slightly higher reformer efficiency, it also has a slightly higher cycle efficiency (Figure 13).

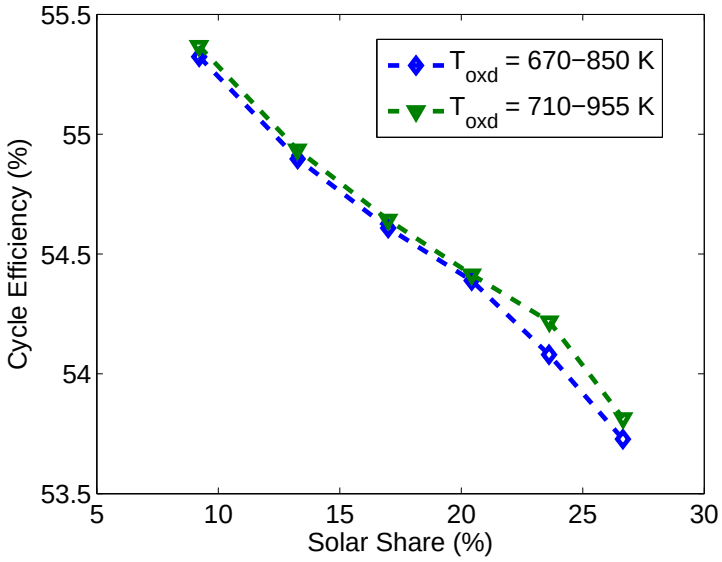

Figure 13: Cycle Efficiency at Different Oxidation Temperatures

Similar to previous studies, the reformer and cycle efficiencies again decrease with increasing solar share.

To summarize, increasing the oxidation temperature does lead to slightly higher reformer and cycle efficiency. However, since the difference in reformer and cycle performance is not that significant, the lower temperature case might be preferred due to lower costs associated with lower temperature solar receivers. The effect of oxidation temperature is similar for both the steam redox reformer cycle and CO_2 redox reformer cycle in that increasing the oxidation temperature leads to both better reformer and cycle performance [18]. Note that the increase in reformer and cycle performance is more significant in the steam redox reformer case.

Now that the effect of important parameters on reformer and cycle performance and the difference in effect of parameters between the CO_2 redox reformer cycle analyzed herein and the steam redox reformer cycle analyzed in [18] have been pre-

sented, the comparison between CO_2 redox and steam redox reformer hybrid cycle performance will be discussed.

4.4. Comparison of Reformer and Cycle Performance for steam redox and CO_2 redox hybrid cycles

Similar to the comparison of the effect of parameters presented before, for comparison between the performance of the steam redox and CO_2 redox reformer hybrid cycles, the results from [18] will be used for the steam redox reformer hybrid cycle. For an accurate comparison of reformer and cycle performance the operating conditions for the two cycles should be as similar as possible. In this comparison, the amount of reforming steam or CO_2 used is set to 0.250 kmol/s (approximately 2 times stoichiometric since more than stoichiometric amounts of CO_2 is needed to fully convert the iron at reasonable temperatures - see Figure 3). The reformer pressure is set to 20 bar. For the oxidation temperature, the case where solar is used for both the reduction and oxidations is used for the steam redox reformer and the higher oxidation temperature case is used for the CO_2 redox reformer. These cases were chosen to have as close to the same oxidation temperature as possible.

The comparison of the reformer efficiency for the steam redox and CO_2 redox reformer is shown in Figure 14. The CO_2 redox reformer has a higher reformer efficiency than the steam redox reformer despite the lower reduction reactor temperature and lower methane conversion (Figure 15). The reason for the lower temperatures in the CO_2 redox case is because there is less solar energy available for the reduction reactor because more of the solar energy is used for the oxidation reactor as it is needed in order to achieve the necessary temperatures for complete conversion of metal.

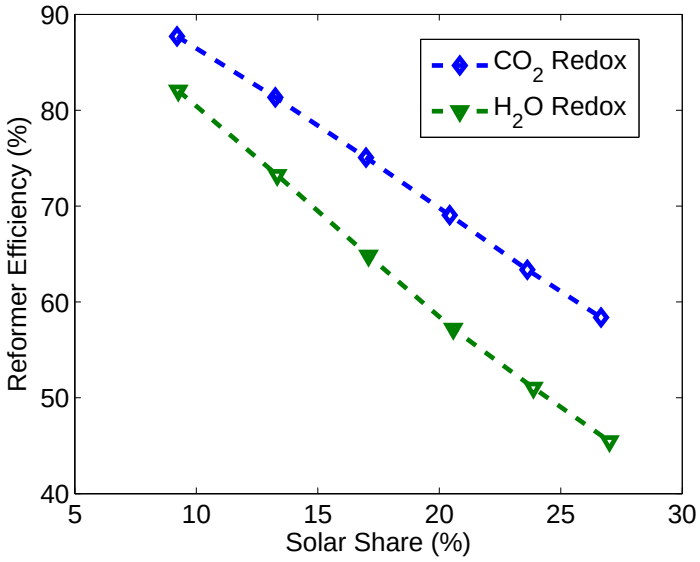

Figure 14: Reformer Efficiency Comparison between CO_2 and Steam Redox Reformer

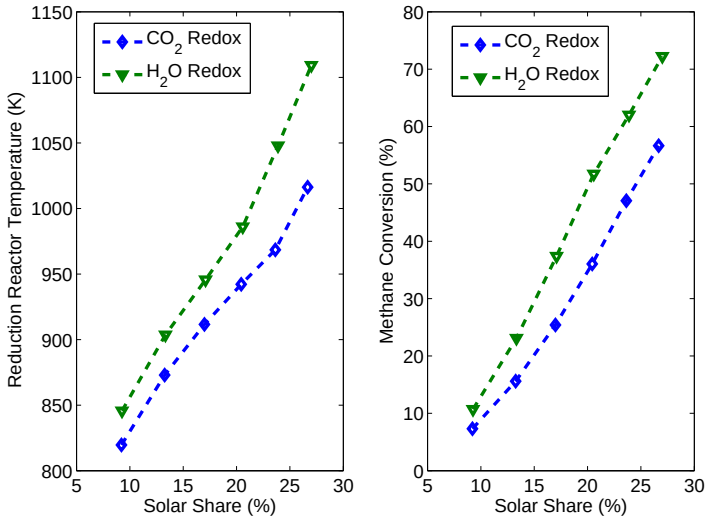

Figure 15: Reduction Reactor Temperature and Methane Conversion Comparison between CO_2 and Steam Redox Reformer

However, since the oxidation reaction with CO_2 is endothermic rather than exothermic (as is the case with steam), there is additional solar "storage" in the oxidation reactor for the CO_2 system that is not there for the steam system. Thus, despite the lower methane conversion, the CO_2 system has the higher reformer efficiency due to the additional "storage" capacity within the oxidation reaction.

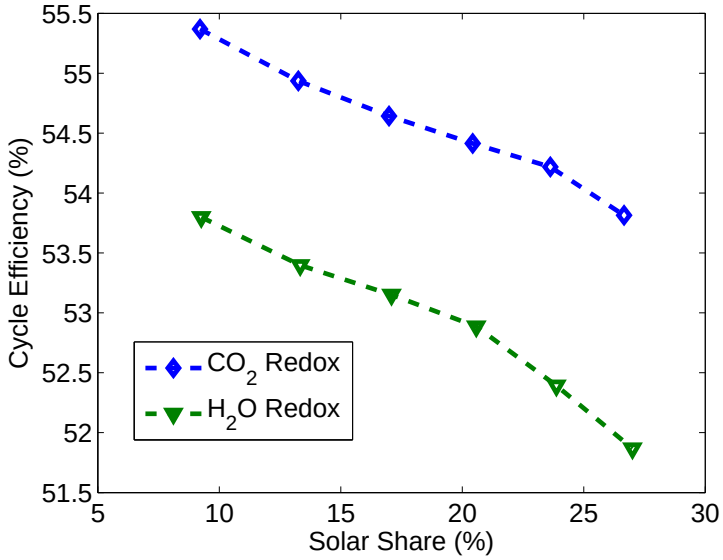

Figure 16: Cycle Efficiency Comparison between CO_2 and Steam Redox Reformer Cycles

The cycle efficiency comparison between the steam redox and CO_2 redox reformer hybrid cycle is shown in Figure 16. Since the CO_2 redox reformer has a higher reforming efficiency, the cycle efficiency is higher for the CO_2 redox reformer hybrid cycle (despite lower reduction reactor temperatures/lower methane conversions). Another contributing factor is that since steam is not being used in the CO_2 redox reformer, more steam is used to produce power within the steam turbines rather than for reforming. Moreover, the excess CO_2 from the redox reformer can be used to produce more power from the gas turbine while the excess steam from the redox reformer

cannot. Also note that the decrease in cycle efficiency with increasing solar share is not as steep for the CO_2 redox cycle.

A summary of the comparison between the CO_2 redox and steam redox hybrid cycles is shown in Table 3.

	CO_2 Redox	**Steam Redox [18]**
Oxidation reaction conditions	Endothermic - favors higher temperatures (requires super stoichiometric amounts of CO_2)	Exothermic - favors lower temperatures
Effect of pressure	Does not affect reformer efficiency, increases cycle efficiency	Does not affect reformer efficiency, increases cycle efficiency
Effect of amount of reforming CO_2/H_2O	Increasing CO_2 increases both reformer and cycle efficiency	Increasing H_2O increases reformer efficiency but not much effect on cycle efficiency
Effect of oxidation temperature	Higher oxidation temperature slightly increases both reformer and cycle efficiency	Higher oxidation temperature greatly increases both reformer and cycle efficiency
Comparison of reformer and cycle efficiency	For a large range of solar shares, the CO_2 redox has higher reformer and cycle efficiency	

Table 3: Summary of Comparison between CO_2 and Steam Redox Hybrid Cycles

5. Conclusion

In summary, system level analysis shows the effect of various operating parameters, including reformer pressure, oxidation temperature, and CO_2 to fuel ratio, on both reformer and cycle performance. Increasing the reformer operating pressure does not have much effect on reformer efficiency. However, increasing the pressure does improve the cycle efficiency to a certain extent. Increasing the amount of reforming CO_2 used does improve both reformer and cycle efficiency; however it should be noted that this could potentially increase the cost of the hybrid cycle. For the oxidation temperature, increasing the oxidation temperature increases both the reformer and cycle efficiency. Comparison of the CO_2 redox reforming cycle to the steam redox reforming cycle analyzed previously in [18] shows that the CO_2 redox reforming cycle has both a higher reformer and cycle efficiency for a large range of solar shares.

While the analysis shows that using a CO_2 redox reformer within a hybrid cycle has potential and can possibly yield better performance than the steam redox reformer, there are other issues that were not considered including size of reactors required and the potentially higher amount of CO_2 capture that would be needed in the CO_2 redox reformer hybrid cycle. Moreover, the CO_2 redox reformer hybrid cycle requires a pure CO_2 stream which may or may not be feasible. Additionally, while the steam redox reformer can be operated with a stoichiometric amount of reforming steam, the CO_2 redox reformer cannot be operated with a stoichiometric amount of reforming CO_2. All these aspects could make the steam redox reformer a more economically viable option for hybrid cycles than the CO_2 redox reformer. Nonetheless, the analysis performed herein illustrates the effect of important operating parameters on CO_2 redox reformer and hybrid cycle performance and also shows

that CO_2 redox reformer hybrid cycles can potentially have better performance than steam redox reformer hybrid cycles.

Acknowledgment

The authors would like to thank the King Fahd University of Petroleum and Minerals in Dhahran, Saudi Arabia, for funding the research reported in this article through the Center for Clean Water and Clean Energy at MIT and KFUPM under project number R12-CE-10. Aspen Plus® was generously provided by Aspen Technology.

References

[1] International Energy Outlook 2013. Tech. Rep.; U.S. Energy Information Administration; 2013.

[2] Sheu, E.J., Mitsos, A., Eter, A.A., Mokheimer, E.M.A., Habib, M.A., Al-Qutub, A.. A review of hybrid solar-fossil fuel power generation systems and performance metrics. ASME Journal of Solar Energy Engineering 2012;134(4):041006:1–17.

[3] Sheu, E.J., Mitsos, A.. Optimization of a hybrid solar-fossil fuel plant: Solar steam reforming of methane in a combined cycle. Energy 2013;51:193–202.

[4] Anikeev, V., Bobrin, A., Ortner, J., Schmidt, S., Funken, K.H., Kuzin, N.. Catalytic thermochemical reactor/receiver for solar reforming of natural gas: Design and performance. Solar Energy 1998;63(2):97 – 104.

[5] Berman, A., Karn, R.K., Epstein, M.. Steam reforming of methane on a Ru/Al_2O_3 catalyst promoted with mn oxides for solar hydrogen production. Green Chem 2007;9:626–631.

[6] Buck, R., Muir, J.F., Hogan, R.E.. Carbon dioxide reforming of methane in a solar volumetric receiver/reactor: the CAESAR project. Solar Energy Materials 1991;24(14):449 – 463.

[7] Maria, G.D., Tiberio, C., D'Alessio, L., Piccirilli, M., Coffari, E., Paolucci, M.. Thermochemical conversion of solar energy by steam reforming of methane. Energy 1986;11(8):805 – 810.

[8] Dahl, J.K., Weimer, A.W., Lewandowski, A., Bingham, C., Bruetsch, F., Steinfeld, A.. Dry reforming of methane using a solar-thermal aerosol flow reactor. Industrial & Engineering Chemistry Research 2004;43(18):5489–5495.

[9] Levy, M., Rubin, R., Rosin, H., Levitan, R.. Methane reforming by direct solar irradiation of the catalyst. Energy 1992;17(8):749 – 756.

[10] Tamme, R., Buck, R., Epstein, M., Fisher, U., Sugarmen, C.. Solar upgrading of fuels for generation of electricity. Journal of Solar Energy Engineering 2001;123(2):160–163.

[11] Wörner, A., Tamme, R.. CO_2 reforming of methane in a solar driven volumetric receiver reactor. Catalysis Today 1998;46(23):165 – 174.

[12] Kodama, T., Ohtake, H., Matsumoto, S., Aoki, A., Shimizu, T., Kitayama, Y.. Thermochemical methane reforming using a reactive WO_3/W redox system. Energy 2000;25(5):411 – 425.

[13] Loutzenhiser, P.G., Meier, A., Steinfeld, A.. Review of the two-step h2o/co2-splitting solar thermochemical cycle based on zn/zno redox reactions. Materials 2010;3(11):4922–4938.

[14] Solunke, R.D., Veser, G.. Hydrogen production via chemical looping steam reforming in a periodically operated fixed-bed reactor. Industrial & Engineering Chemistry Research 2010;49(21):11037–11044.

[15] Steinfeld, A., Brack, M., Meier, A., Weidenkaff, A., Wuillemin, D.. A solar chemical reactor for co-production of zinc and synthesis gas. Energy 1998;23(10):803 – 814.

[16] Steinfeld, A., Kuhn, P., Karni, J.. High-temperature solar thermochemistry: Production of iron and synthesis gas by Fe_3O_4-reduction with methane. Energy 1993;18(3):239 – 249.

[17] Yamaguchi, D., Tang, L., Burke, N., Chiang, K., Rye, L., Hadley, T., et al. Hydrogen Energy: Challenges and Perspectives; chap. 2. Intech; 2012, p. 31–54.

[18] Sheu, E.J., Ghoniem, A.F.. Redox reforming based, integrated solar-natural gas plants: Reforming and thermodynamic cycle efficiency. International Journal of Hydrogen Energy 2014;39(27):14817 – 14833.

[19] Barin, I., Sauert, F., Schultze-Rhonhof, E., Sheng, W.S.. Thermochemical Data of Pure Substances. VCH Verlagsgesellschaft mbH; 1993.

[20] Steinfeld, A., Meier, A.. Solar fuels and materials. In: in Chief: Cutler J. Cleveland, E., editor. Encyclopedia of Energy. New York: Elsevier; 2004, p. 623 – 637.